Renal tubular NEDD4-2 deficiency causes NCC-mediated salt-dependent hypertension

Caroline Ronzaud,[1] Dominique Loffing-Cueni,[2] Pierrette Hausel,[1] Anne Debonneville,[1] Sumedha Ram Malsure,[1] Nicole Fowler-Jaeger,[1] Natasha A. Boase,[3] Romain Perrier,[1] Marc Maillard,[4] Baoli Yang,[5] John B. Stokes,[6] Robert Koesters,[7] Sharad Kumar,[3] Edith Hummler,[1] Johannes Loffing,[2] and Olivier Staub[1]

[1]Department of Pharmacology and Toxicology, University of Lausanne, Lausanne, Switzerland. [2]Institute of Anatomy, University of Zurich, Zurich, Switzerland. [3]Department of Hematology, Centre for Cancer Biology, Adelaide, Australia. [4]Nephrology Department, Centre Hospitalier Universitaire Vaudois (CHUV), Lausanne, Switzerland. [5]Department of Obstetrics and Gynecology, University of Iowa, Iowa City, Iowa, USA. [6]Department of Internal Medicine, University of Iowa, and VA Medical Center, Iowa City, Iowa, USA. [7]INSERM UMRS 702, UPMC, Tenon Hospital, Paris, France.

The E3 ubiquitin ligase NEDD4-2 (encoded by the *Nedd4L* gene) regulates the amiloride-sensitive epithelial Na^+ channel (ENaC/SCNN1) to mediate Na^+ homeostasis. Mutations in the human β/γENaC subunits that block NEDD4-2 binding or constitutive ablation of exons 6–8 of *Nedd4L* in mice both result in salt-sensitive hypertension and elevated ENaC activity (Liddle syndrome). To determine the role of renal tubular NEDD4-2 in adult mice, we generated tetracycline-inducible, nephron-specific *Nedd4L* KO mice. Under standard and high-Na^+ diets, conditional KO mice displayed decreased plasma aldosterone but normal Na^+/K^+ balance. Under a high-Na^+ diet, KO mice exhibited hypercalciuria and increased blood pressure, which were reversed by thiazide treatment. Protein expression of βENaC, γENaC, the renal outer medullary K^+ channel (ROMK), and total and phosphorylated thiazide-sensitive Na^+Cl^- cotransporter (NCC) levels were increased in KO kidneys. Unexpectedly, *Scnn1a* mRNA, which encodes the αENaC subunit, was reduced and proteolytic cleavage of αENaC decreased. Taken together, these results demonstrate that loss of NEDD4-2 in adult renal tubules causes a new form of mild, salt-sensitive hypertension without hyperkalemia that is characterized by upregulation of NCC, elevation of β/γENaC, but not αENaC, and a normal Na^+/K^+ balance maintained by downregulation of ENaC activity and upregulation of ROMK.

Introduction

Hypertension is a major risk factor for stroke, myocardial infarction, and heart and kidney failure. The postmacula densa segments of the nephron, namely the distal convoluted tubule (DCT), the connecting tube (CNT) and the collecting duct (CD), control Na^+ and K^+ balance and thus extracellular volume and blood pressure. Na^+ reabsorption occurs in the DCT by electroneutral cotransport via the thiazide-sensitive Na^+Cl^- cotransporter (NCC) and in the late portion of the DCT (DCT2), CNT, and CD by electrogenic Na^+ reabsorption through the amiloride-sensitive epithelial Na^+ channel (ENaC) (1). ENaC provides the driving force for K^+ secretion via the renal outer medullary K^+ channel (ROMK) (2).

The significance of these 3 renal segments for controlling Na^+ balance and blood pressure is underscored by genetic diseases affecting ENaC and NCC. Gain-of-function mutations within *SCNN1* cause Liddle syndrome, which is characterized by increased ENaC activity, and result in salt retention and hypertension (3). Such mutations in β- and γENaC lead to inactivation of the PY motif that interacts with WW domains of the ubiquitin-protein ligase NEDD4-2 (encoded by the *Nedd4L* gene), which ubiquitylates and degrades the channel (4–8). With increased aldosterone secretion, serum- and glucocorticoid-regulated kinase 1 (SGK1) interferes with ENaC ubiquitylation by NEDD4-2 (9). In addition, ENaC has been shown to be activated by proteolytic cleavage of the α and γ subunits that reflects ENaC activation and leads to channel with a higher open probability (10–12). Moreover, the α subunit is needed to bring β- and γENaC to the apical membrane, making functional channels (13–15).

The activity of NCC plays a major role in Na^+ balance and blood pressure regulation. Thiazide diuretics, which inhibit NCC and lower blood pressure, and genetic mutations that suppress or heighten NCC function cause hypotension or hypertension, respectively (16). NCC is also a downstream molecular target of the with-no-lysine WNK1/WNK4 kinases (17, 18), the kelch-like KLHL3/Cullin 3 (CUL3) ubiquitin-protein ligase complex (19, 20), and the SGK1 kinase (21). Mutations in human proteins lead to overactive NCC and cause pseudohypoaldosteronism type II (PHAII) (19, 20, 22), characterized by hyperkalemia, hypertension, hypercalciuria, and metabolic acidosis that can be treated by thiazides (23). Very recently, we have shown both in vitro and in vivo that Nedd4-2 is involved in NCC regulation (24).

Generation of constitutive *Nedd4L* KO mice, by removing exons 6 to 8 of the *Nedd4L* gene (*Nedd4L*-Δ*6-8* KO mice), demonstrated the importance of NEDD4-2 in the control of ENaC activity and blood pressure (25). Indeed, these mice displayed impaired Na^+ excretion and hypertension, apparently mediated by ENaC overactivity (25). No effect on NCC was observed. To determine the role of renal NEDD4-2 in controlling Na^+ balance and blood pressure during adulthood and to dissect the mechanisms behind this regulation, we developed inducible renal tubule–specific $Nedd4L^{flox/flox}$/*Pax8-rTA/LC1* KO mice ($Nedd4L^{Pax8/LC1}$). Here, we show that loss of *Nedd4L* in adult renal tubules leads to some

Authorship note: Johannes Loffing and Olivier Staub contributed equally to this work. John B. Stokes is deceased.

Conflict of interest: The authors have declared that no conflict of interest exists.

Citation for this article: *J Clin Invest.* 2013;123(2):657–665. doi:10.1172/JCI61110.

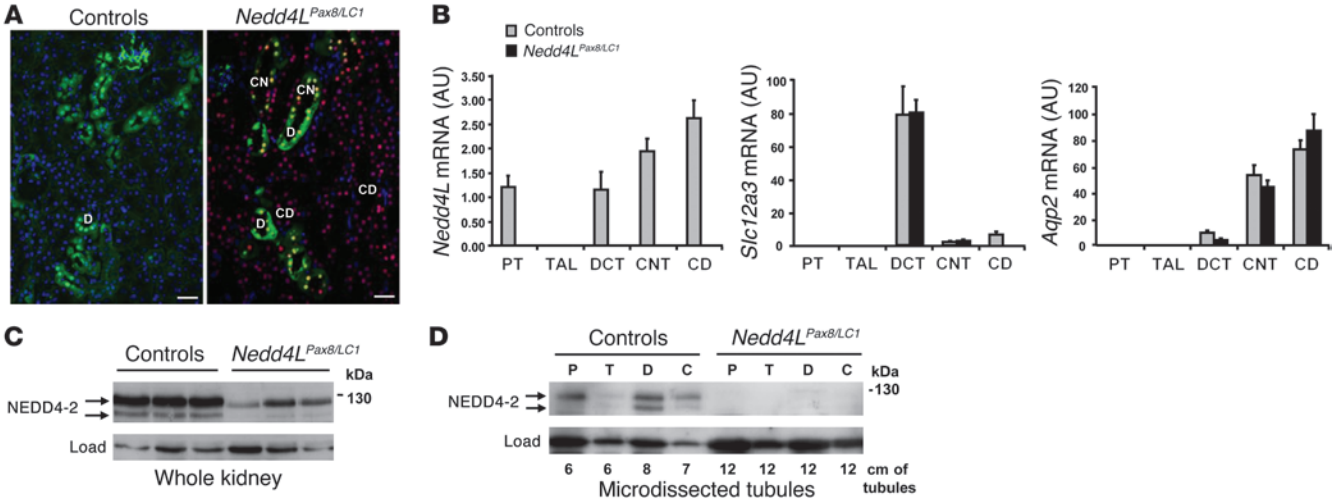

Figure 1

Generation of inducible renal tubule–specific *Nedd4L* KO mice. *Nedd4L*$^{flox/flox}$/*Pax8-rTA*/*LC1* KO mice and control littermates (*Nedd4L*^{Pax8} or *Nedd4L*^{LC1}) were obtained and treated with doxycycline as described previously (24) to induce *Nedd4L* ablation in renal tubular cells. (**A**) Immunofluorescence for CRE and calbindin CaBP28 on kidney sections from control (left panel) and induced *Nedd4L*$^{Pax8/LC1}$ KO (right panel). CRE recombinase is expressed in all renal tubules in induced KO mice, including CaBP28-positive DCT/CNT cells (CRE: red; CaBP28: green; DAPI: blue). Scale bars: ~50 μm. C, CNT; D, DCT. (**B**) Quantitative real-time PCR analysis for *Nedd4L*, *Slc12a3* (encoding NCC), and aquaporin 2 (*Aqp2*) mRNA on microdissected renal tubules normalized to *Gapdh*: *Nedd4L* mRNA is not detected in *Nedd4L*$^{Pax8/LC1}$ KO, and *Slc12a3* mRNA levels are unchanged (n = 4 per group, 8 days of high-Na$^+$ diet). *Slc12a3* was used as DCT marker and *Aqp2* as CNT/CD marker. (**C** and **D**) Analysis of NEDD4-2 protein expression by Western blot in whole kidney lysates (**C**) and microdissected tubules (**D**). The lower NEDD4-2 expression observed in KO whole-kidney lysates is absent in microdissected tubules (n = 3 mice per genotype). Load: unspecific band used as loading control. C, CNT/CD; P, PT; T, TAL.

features of salt-sensitive PHAII with overactive NCC, leading to increased blood pressure and hypercalciuria. Interestingly, compensation by increased ROMK abundance and downregulation of ENaC activity allows the maintenance of a normal Na$^+$/K$^+$ balance.

Results

Generation of inducible renal tubule–specific Nedd4L KO mice. Germline deletion of exons 6 to 8 of the *Nedd4L* gene in mice leads to ENaC overactivation and hypertension (25). To determine the role of renal NEDD4-2 in regulating Na$^+$ balance and blood pressure in adult mice, we generated inducible renal tubule–specific *Nedd4L* KO mice using the same floxed allele used previously (25) and a combination of the inducible Tet-On and Cre-loxP systems, as previously described (24). Double-transgenic *Nedd4L*$^{flox/flox}$/*Pax8-rTA/LC1* (*Nedd4L*$^{Pax8/LC1}$) conditional KO mice and single-transgenic *Nedd4L*$^{flox/flox}$/*Pax8-rTA* (*Nedd4L*^{Pax8}) or *Nedd4L*$^{flox/flox}$/*LC1* (*Nedd4L*^{LC1}) control littermates were treated with doxycycline as described previously (24). Immunofluorescence analysis showed that Cre recombinase is expressed in every tubular cell along the renal tubules of doxycycline-treated KO, but not in the blood vessels (Figure 1A). Consistent with previous report (26), *Nedd4L* mRNA could be detected in the proximal tubule (PT), DCT, CNT, and CD in microdissected tubules of control mice, but not in KO (Figure 1B). Western blot on total kidney lysates revealed a decrease of the 130-kDa NEDD4-2 protein in doxycycline-treated KO mice (Figure 1C). Using several antibodies against NEDD4-2, we observed that the remaining band at 130 kDa was consistently present at low levels in the KO mice (Supplemental Figure 1; supplemental material available online with this article; doi:10.1172/JCI61110DS1). However, this band was completely lost when Western blots were performed on microdissected tubules (Figure 1D). These data indicate that the lower expression of NEDD4-2 observed on whole kidney extracts of KO mice corresponds to NEDD4-2 expressed in nontubular cells that were not targeted using the Pax8-rTA/LC1 system. Moreover, no additional truncated NEDD4-2 protein could be detected with the existing NEDD4-2 antibodies in the KO. As it was previously reported that the Pax8-rTA/LC1-mediated recombination system was leaky in some hepatocytes (27), we performed PCR to check the presence of recombination in liver and observed a weak band corresponding to the *Nedd4L* null allele in the KO (Supplemental Figure 2A). However, immunoblotting on whole KO liver showed normal NEDD4-2 protein expression in the KO (Supplemental Figure 2B). NEDD4-1 protein, closely related to NEDD4-2 (28), was not upregulated in the *Nedd4L*$^{Pax8/LC1}$ KO mice, indicating that there is no compensation by this paralogue (Supplemental Figure 3).

Nedd4L$^{Pax8/LC1}$ *KO mice show normal urine and plasma Na$^+$ and K$^+$ levels.* Control and KO mice were fed with a standard or high-Na$^+$ diet and placed in metabolic cages to analyze Na$^+$/K$^+$ balance. Plasma aldosterone levels were strongly decreased in the KO mice under both diets, suggesting increased Na$^+$ retention (Figure 2A). However, KO did not show any change in plasma Na$^+$ and K$^+$ concentrations (Table 1). Moreover, after a change from standard to high-Na$^+$ diet, KO mice showed a tendency to retain Na$^+$ compared with controls, but this was not statistically significant (Supplemental Figure 4). These data indicate either that the *Nedd4L*$^{Pax8/LC1}$ KO mice are able to maintain a normal Na$^+$/K$^+$ balance or that they have a modest Na$^+$ retention that could not be detected by measuring urinary Na$^+$ excretion. Interestingly, when fed with a high-Na$^+$

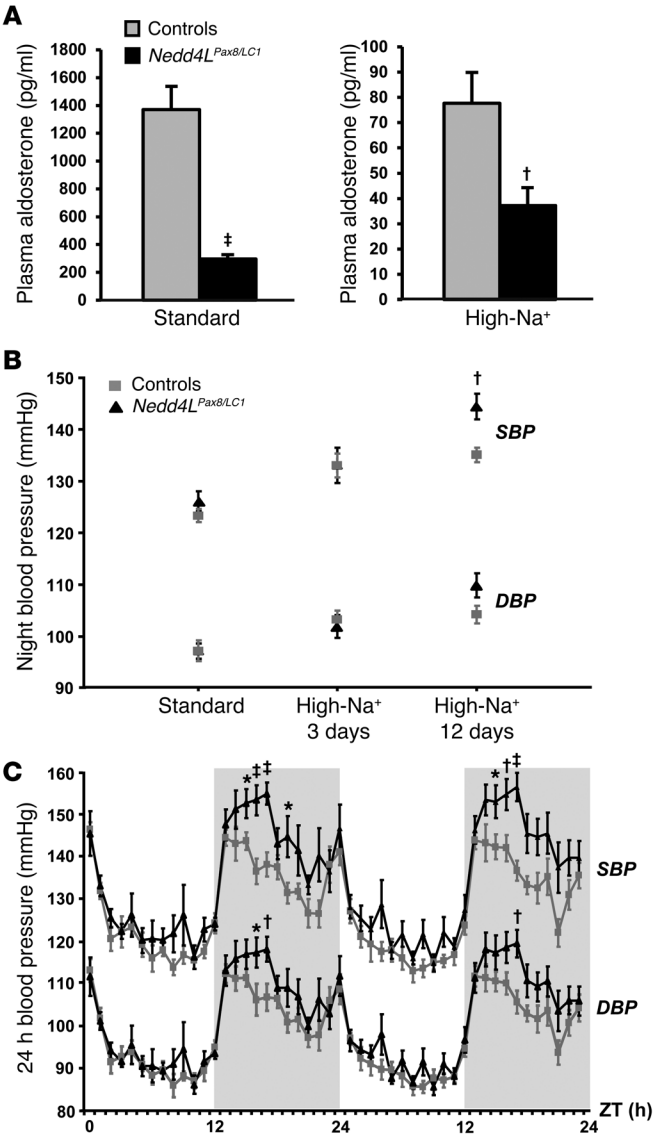

Figure 2
Inducible *Nedd4L*$^{Pax8/LC1}$ KO mice show decreased plasma aldosterone and salt-sensitive blood pressure increase. (**A**) Plasma aldosterone levels were decreased in induced *Nedd4L*$^{Pax8/LC1}$ KO (n = 7–10) compared with controls (n = 6–9) under both standard and high-Na$^+$ diets. (**B**) Graphs represent SBP and DBP 12-hour night averages measured by telemetry in controls (n = 8) and *Nedd4L*$^{Pax8/LC1}$ KO (n = 6) under standard diet and after 3 and 12 days of high-Na$^+$ diet. (**C**) SBP and DBP 24-hour profiles (day, white zone; night, gray zone) in controls (gray curve) and *Nedd4L*$^{Pax8/LC1}$ KO (black curve) after 12 days of high-Na$^+$ diet. ZT, Zeitgeber time (ZT0 or ZT24, light on; ZT12, light off). $^*P < 0.05$, $^\dagger P < 0.01$, $^\ddagger P < 0.005$, KO versus controls.

diet, KO mice displayed increased water consumption, elevated urine output, and diluted urine (Table 1), as previously observed in constitutive *Nedd4L-Δ6-8* KO mice (25).

Loss of renal tubule NEDD4-2 in adult mice leads to salt-sensitive blood pressure increase. Systolic and diastolic arterial blood pressures (SBP and DBP) were measured by telemetry for 3 consecutive 24-hour periods upon standard and high-Na$^+$ diets. No significant difference between *Nedd4L*$^{Pax8/LC1}$ KO and control littermates was observed under standard diet (Figure 2B). However, following 12 days of high-Na$^+$ diet, the difference between controls and KO reached 10 mmHg for the SBP during the active night period (Figure 2, B and C). These data indicate that renal tubule NEDD4-2 in adult mice is important for maintaining normal blood pressure under high-salt intake.

Nedd4L inactivation in adult renal tubules leads to increased β- and γENaC protein expression, but reduced αENaC proteolysis. Because NEDD4-2 has been shown to participate in the degradation of ENaC, it was expected that *Nedd4L* inactivation would result in more ENaC expression. Immunofluorescence showed that both β- and γENaC are strongly increased in *Nedd4L*$^{Pax8/LC1}$ KO renal tubules (Figure 3, B and C, and Supplemental Figure 5). However, the cellular localization of both subunits was mainly cytoplasmic. Interestingly, αENaC expression was not increased in KO mice and seen predominantly at intracellular sites (Figure 3A and Supplemental Figure 5). Consistently, *Scnn1a* mRNA levels were lower in microdissected tubules of KO mice that paralleled the decreased plasma aldosterone levels observed in these mice (Figure 3D). On the other hand, *Scnn1b* and *Scnn1g* mRNA expression was unchanged (Figure 3, E and F). It is known that proteolytic cleavage of the α and γ subunits is involved in ENaC activation (10, 12, 29). We therefore analyzed by immunoblotting whether loss of NEDD4-2 would affect ENaC cleavage. *Nedd4L*$^{Pax8/LC1}$ KO mice showed a strong increase in the 90-kDa band for βENaC (Figure 3H). The same was observed for γENaC, but no 70-kDa cleaved form could be detected (Figure 3H). For αENaC, there was no change in the expression of the 90-kDa uncleaved band (quantification of blots from 3 independent experiments: controls: 1.00 ± 0.22, n = 16; KO: 0.94 ± 0.18, n = 17; P = 0.818), but the 30-kDa cleaved band was decreased in the KO (controls: 1.00 ± 0.20, n = 16; KO: 0.48 ± 0.13, n = 17; P = 0.044) (Figure 3G). When aldosterone was administered to the *Nedd4L*$^{Pax8/LC1}$ KO mice using osmotic minipumps, both uncleaved and cleaved forms of αENaC expression increased and achieved comparable levels to those in the controls (Figure 3I). These results indicate that the downregulation of the αENaC proteolytic cleavage is due to decreased aldosterone. Taken together, our data suggest that ENaC activity is downregulated in *Nedd4L*$^{Pax8/LC1}$ KO mice.

Loss of renal tubule NEDD4-2 in adult mice leads to overactive NCC. We have recently showed that NEDD4-2 is involved in the regulation of NCC at the posttranslational level (24). Here, we confirm, by using immunofluorescence, that loss of NEDD4-2 leads to increased NCC protein abundance (Figure 4A) without any change of *Slc12a3* mRNA expression in microdissected renal tubules (Figure 1B). NCC immunostaining was hardly visible in control mice fed a high-Na$^+$ diet, while an immunofluorescent signal was easily detectable in the KO mice. Immunoblotting data indicated that the elevated NCC phosphorylation at T53, T58, and S71, known to be involved in the activation of the cotransporter, followed the increased NCC protein abundance in KO (ref. 30 and Figure 4, B and C). To confirm our observation, we looked at NCC expression in kidneys from P19 *Nedd4L-Δ15-16* KO mice generated by Boase et al. (31) and observed an increase of expression and phosphorylation of the cotransporter also in these mice (Supplemental Figure 6). Thus, we confirm that loss of NEDD4-2 leads to increased NCC. PHAII patients and mouse models with overactive NCC dis-

Table 1
Urine and plasma electrolytes in controls and inducible *Nedd4L*$^{Pax8/LC1}$ KO mice under standard and high-Na$^+$ diet (8 days)

	Standard diet		High-Na$^+$ diet	
	Controls	***Nedd4L*$^{Pax8/LC1}$**	**Controls**	***Nedd4L*$^{Pax8/LC1}$**
Food intake (g/g BW/24 h)	0.13 ± 0.00 (7)	0.15 ± 0.01 (4)	0.18 ± 0.01 (18)	0.17 ± 0.01 (15)
Water intake (ml/g BW/24 h)	0.31 ± 0.04 (7)	0.36 ± 0.03 (4)	0.32 ± 0.01 (21)	0.39 ± 0.02^B (15)
Urine				
Urine volume (ml/24 h)	0.13 ± 0.01 (7)	0.14 ± 0.02 (4)	0.13 ± 0.01 (21)	0.17 ± 0.01^A (15)
Osmolality (mmol/g H_2O)	ND	ND	2541 ± 204 (10)	1791 ± 72^A (9)
Na$^+$ excretion (μmol/24 h)	150 ± 15.8 (7)	187 ± 9.84 (4)	1375 ± 204 (10)	1352 ± 154 (14)
Na$^+$/Cr (10^3)	0.03 ± 0.00 (7)	0.05 ± 0.01 (4)	0.59 ± 0.06 (7)	0.55 ± 0.08 (4)
K$^+$ excretion (μmol/24 h)	520 ± 51.8 (7)	609 ± 71.7 (4)	428 ± 29.4 (21)	438 ± 30.2 (14)
K$^+$/Cr (10^3)	0.10 ± 0.01 (7)	0.16 ± 0.02 (4)	0.14 ± 0.01 (7)	0.13 ± 0.02 (4)
Na$^+$/K$^+$	0.27 ± 0.02 (7)	0.32 ± 0.03 (4)	3.07 ± 0.18 (18)	3.25 ± 0.35 (15)
GFR (ml/g BW/24 h)	14.3 ± 2.69 (7)	17.6 ± 3.30 (4)	12.9 ± 3.10 (8)	11.1 ± 0.87 (6)
pH	6.08 ± 0.04 (7)	6.17 ± 0.00 (4)	5.81 ± 0.20 (4)	5.91 ± 0.21 (6)
Plasma				
Na$^+$ (mM)	150 ± 1.26 (7)	147 ± 1.35 (4)	151 ± 1.14 (15)	151 ± 1.43 (11)
K$^+$ (mM)	5.35 ± 0.29 (7)	6.19 ± 1.12 (4)	4.71 ± 0.19 (10)	4.72 ± 0.19 (10)
Blood pH	ND	ND	7.55 ± 0.04 (5)	7.58 ± 0.04 (7)

Values are given as average ± SEM. Number of mice indicated in parentheses. Cr, creatinine. $^AP < 0.05$, $^BP < 0.005$, KO versus controls.

play hypercalciuria that can be treated by thiazides, whereas hypocalciuria is observed in *Slc12a3* KO mice (32). NCC activity is thus correlated with renal Ca^{2+} excretion. Based on this observation, we measured the urinary Ca^{2+} and found that the *Nedd4L*$^{Pax8/LC1}$ KO excrete more Ca^{2+} under a high-Na$^+$ diet. Interestingly, thiazide treatment markedly reduced the elevated Ca^{2+} excretion in the KO, similar to what occurs in PHAII patients (Figure 4D). In addition, thiazide, but not amiloride, decreased the difference in blood pressure between controls and KO during the active night period (Figure 4E). Taken together, these data suggest that loss of NEDD4-2 in renal tubules in adult mice leads to increased NCC activity.

Nedd4L$^{Pax8/LC1}$ *KO mice have increased ROMK abundance.* Increased NCC activity has been shown to be linked with K$^+$ retention (33, 34). Therefore, the absence of hyperkalemia in *Nedd4L*$^{Pax8/LC1}$ KO mice was unexpected, as they do also show decreased ENaC activity and plasma aldosterone that should decrease the electrochemical driving force for K$^+$ excretion via apical K$^+$ channels such as ROMK in the ENaC-expressing cells. We therefore analyzed the abundance and subcellular localization of ROMK in control and KO mice. Interestingly, immunofluorescence showed a strong increase in ROMK protein abundance and apical localization in the DCT and CNT of *Nedd4L*$^{Pax8/LC1}$ KO (Figure 5A) and in CD and thick ascending limb (TAL) (Figure 5A). *Kcnj1* mRNA expression levels (Figure 5B) were not different between controls and KO, indicating that loss of NEDD4-2 affects ROMK expression at the posttranslational level.

Nedd4L ablation in renal tubules during embryonic development results in a phenotype similar to that seen when the deletion occurs at adult age. Because the total *Nedd4L*-Δ*6-8* KO mice showed no change in plasma aldosterone under standard and high-Na$^+$ diets, increase in αENaC expression, and no alteration of NCC abundance (25), we hypothesized that the time of *Nedd4L* deletion may account for the differences with the *Nedd4L*$^{Pax8/LC1}$ KO mice. We treated the pregnant mothers of *Nedd4L*$^{Pax8/LC1}$ KO mice and control littermates with doxycycline during gestation to induce deletion during embryonic development, as previously reported (27). We observed that the constitutive *Nedd4L* ablation in renal tubules had effects on NCC and α-, β- and γENaC expression (Figure 6, A–C) similar to those seen when the deletion was induced during adulthood. Moreover, the constitutive *Nedd4L*$^{Pax8/LC1}$ KO mice showed decreased plasma aldosterone (Figure 6D) and hypercalciuria (Table 2). These data suggest that the differences in phenotype between the *Nedd4L*$^{Pax8/LC1}$ KO mice and the total *Nedd4L*-Δ*6-8* KO mice are most likely not due to early developmental adaptation, but rather to nonrenal NEDD4-2 or to the differences in genetic background between these mouse models.

Discussion

Mutations in human β- and γENaC leading to inactivation of the PY motif that interacts with NEDD4-2 WW domains cause Liddle syndrome, characterized by increased ENaC activity, salt retention, and hypertension (3). Surprisingly, constitutive deletion of exons 6 to 8 of the *Nedd4L* gene in the mouse results in amiloride-sensitive salt-induced hypertension, but no sign of volume expansion or impaired Na$^+$/K$^+$ balance (25). These observations raise the question on the role of renal NEDD4-2 in controlling ENaC and blood pressure. To address this issue, we generated inducible renal tubule–specific *Nedd4L* KO (*Nedd4L*$^{Pax8/LC1}$) mice. No *Nedd4L* mRNA corresponding to the deleted region as well as no protein product could be detected in microdissected renal tubules of *Nedd4L*$^{Pax8/LC1}$ KO mice, suggesting that *Nedd4L* is efficiently deleted in the targeted renal tubular cells. Recently, another constitutive *Nedd4L* KO mouse model was generated by constitutively deleting exons 15 and 16 of the *Nedd4L* gene (*Nedd4L*-Δ*15-16* KO mice) (31). Such deletion led to a perinatal lethal lung phenotype in contrast to the *Nedd4L*-Δ*6-8* KO model. Boase et al. provided evidence that production of a partial NEDD4-2 protein product in the lungs of the *Nedd4L*-Δ*6-8* KO may be the reason for the differences between the 2 models (31). Such truncated NEDD4-2 protein product was not detected in kidneys of our *Nedd4L*$^{Pax8/LC1}$ KO mice.

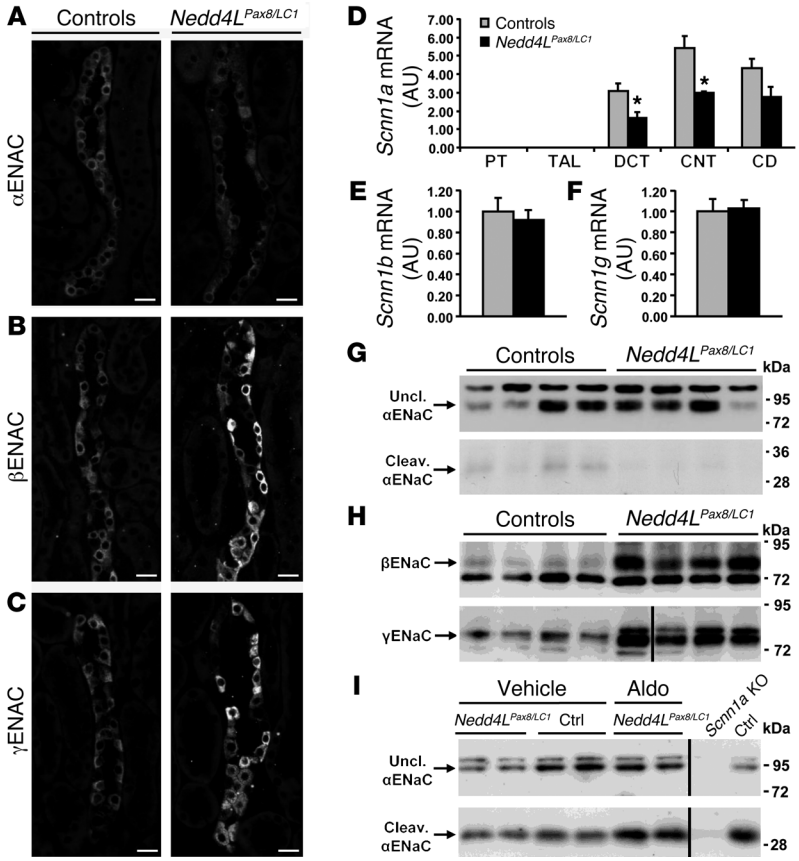

Figure 3

Nedd4L$^{Pax8/LC1}$ KO mice have increased β- and γENaC abundance, but not αENaC. (**A**–**C**) Immunostaining for α- (**A**), β- (**B**), and γENaC (**C**) on kidney cryosections of control and KO mice under high-Na^+ diet. Cytoplasmic β- and γENaC abundance is increased in CD of KO, whereas αENaC is decreased. Scale bars: ~20 μm. (**D**) TaqMan analysis of *Scnn1a* mRNA on microdissected renal tubules shows downregulation in KO (n = 4 per group). (**E** and **F**) TaqMan analysis for *Scnn1b* (**E**) and *Scnn1g* (**F**) mRNA on whole kidney (n = 6 per genotype). mRNA expression was normalized to *Gapdh* mRNA levels and expressed relative to control values. (**G** and **H**) Representative Western blots for α-, β-, and γENaC: the cleaved 30-kDa αENaC band was decreased in *Nedd4L*$^{Pax8/LC1}$ KO mice (**G**), whereas β- and γENaC expression were elevated (**H**). For γENaC, lanes were run on the same gel but were noncontiguous, as indicated by the vertical black line. (**I**) Aldosterone infusion in *Nedd4L*$^{Pax8/LC1}$ KO mice results in increased αENaC protein (uncleaved and cleaved form) expression, suggesting that the reduced expression observed in the KO is due to the decreased plasma aldosterone. Kidney extract from *Scnn1a* KO mice was used as negative control. Lanes that were run on the same gel but were noncontiguous are indicated with the vertical black lines. *P < 0.05, KO versus controls. Ctrl, control mice.

Surprisingly, despite the increase in NCC, and β- and γENaC protein levels and the decreased circulating aldosterone, suggesting Na^+ retention and confirming our previous report (24), *Nedd4L*$^{Pax8/LC1}$ KO mice showed normal urine and plasma Na^+ and K^+ levels. NCC has been reported to be activated by increasing its cell-surface expression and phosphorylation state, mainly via the WNK-SPAK/OSR1 pathway (17, 35). We found that NCC abundance was increased in *Nedd4L*$^{Pax8/LC1}$ KO mice and is accompanied by a proportional increase in phosphorylation of T53, T58, and S71 (30, 35). We also observed that *Nedd4L*$^{Pax8/LC1}$ KO mice have salt-sensitive blood pressure increase and hypercalciuria that could both be corrected by thiazides, corroborating the assumption that the increased NCC is functional. Of interest, thiazides did not completely correct the high blood pressure, suggesting that mechanisms other than NCC activation are likely to contribute. Interestingly, β- and γENaC abundance were increased in the *Nedd4L*$^{Pax8/LC1}$ KO mice, but their cellular localization was mainly intracellular, and γENaC appeared to be in its uncleaved form. Unexpectedly, *Scnn1a* mRNA expression and proteolytic cleavage of the subunit were decreased in the *Nedd4L*$^{Pax8/LC1}$ KO mice, suggesting ENaC downregulation. Moreover, amiloride treatment of *Nedd4L*$^{Pax8/LC1}$ KO mice did not decrease the high blood pressure, indicating that ENaC is not involved in the hypertensive phenotype. Interestingly, the ENaC downregulation observed in the *Nedd4L*$^{Pax8/LC1}$ KO mice paralleled the decreased plasma aldosterone and could be rescued by administrating aldosterone to the KO mice. These data confirm (a) the crucial role of aldosterone in controlling αENaC expression in the kidney (36), and (b) the importance of αENaC for apical trafficking of the 2 other ENaC subunits (37). To our knowledge, this is the first in vivo study showing differential regulation between the upregulation of β/γENaC (a likely result of the lack of ubiquitylation) and the downregulation of proteolytic activation of αENaC due to decreased aldosterone. Interestingly, no human mutation in the gene encoding αENaC (*Scnn1a*) has been reported to cause Liddle syndrome. Taken together, these results give new insights about how the different mechanisms involved in ENaC regulation can interact and compensate each other if one is impaired. However, our results stand in contrast with the phenotype of Liddle syndrome, where ENaC activity is increased despite the low circulating aldosterone levels (38). It is likely that deletion of *Nedd4L* affects other factors, such as NCC upregulation and consequent compensatory pathways, or other factors involved in controlling ENaC activity or trafficking (39). Because modifications in the abundance of individual renal Na^+ transporters often result in compensatory changes in the expression levels of other Na^+ transporters to maintain Na^+ balance (40), we propose that NEDD4-2 deficiency leads to increased NCC-mediated Na^+ reabsorption, which is compensated by decreased ENaC activity. Consistent with our hypothesis, KO mice for the kidney-specific *KS-Wnk1* isoform, in which NCC is strongly upregulated, present a very similar phenotype with downregulation of the 3 ENaC subunits (41). Of interest, the phenotype of the *Nedd4L*$^{Pax8/LC1}$ KO mice is the mirror image of the *Slc12a3* KO, which show increased plasma aldosterone, decreased calciuria, and upregulation of ENaC activity in CD (28).

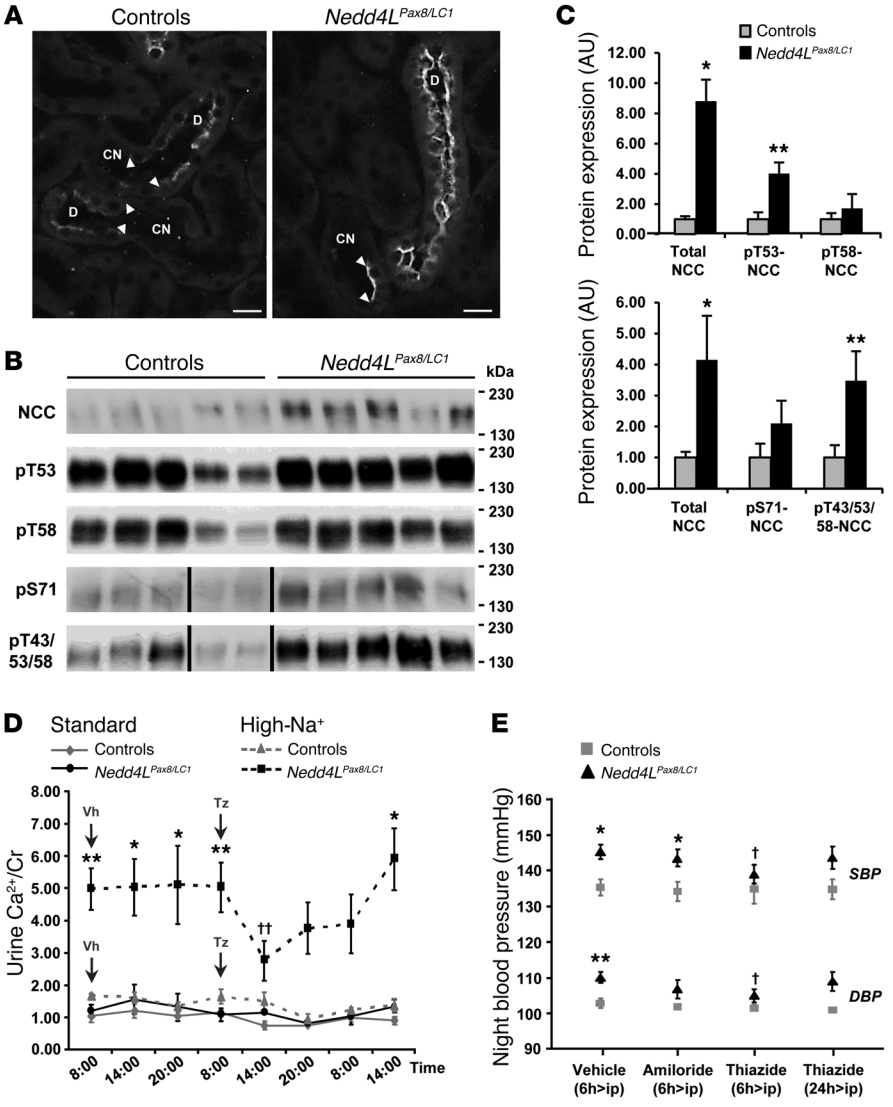

Figure 4

NCC is overactivated in *Nedd4L*$^{Pax8/LC1}$ KO mice. (**A**) Immunofluorescence for NCC on kidney sections of control and KO mice under high-Na$^+$ diet. NCC expression is increased in DCT of KO. Scale bars: ~20 μm. (**B**) Western blot analysis for total NCC and phosphorylated pT53-, pT58-, pS71-, and pT43/53/58-NCC. A representative blot on 5 controls and 5 KO is shown. For pS71-NCC and pT43/53/58-NCC, lanes that were run on the same gel but noncontiguous are indicated with a vertical black line. (**C**) Graphs show quantification of Western blots for phosphorylated NCC and the corresponding total NCC from 2 independent experiments (pT53-NCC and pT58-NCC: $n = 5$ per genotype; pS71-NCC and p43/53/58-NCC: $n = 11$ per genotype). Protein expression was normalized to the amount of β-actin or β-tubulin and expressed relative to control values. (**D**) Urine Ca^{2+} measurement in control and KO mice under high-Na$^+$ diet (10 days). *Nedd4L*$^{Pax8/LC1}$ KO are hypercalciuric as shown by the 3-fold increased urine Ca^{2+}/creatinine (Cr) ratio, which can be corrected by thiazide ($n = 4$ per group). Vh, vehicle; Tz, thiazide. (**E**) Plot showing telemetric measurement on controls versus KO under high-Na$^+$ diet. The increased SBP and DBP observed in KO after 5 weeks of high-Na$^+$ diet can be prevented by thiazide, but not by amiloride ($n = 4$ per group). $^*P < 0.05$, $^{**}P < 0.01$, KO versus controls. $^\dagger P < 0.05$, $^{\dagger\dagger}P < 0.01$, thiazide versus vehicle.

Our results in the *Nedd4L*$^{Pax8/LC1}$ KO mice are however different to what was observed in the total *Nedd4L-Δ6-8* KO mice, in which NCC was unchanged and all 3 ENaC subunits were increased (25). One substantial difference between the 2 models is the plasma aldosterone that is much higher in the total *Nedd4L-Δ6-8* KO mice and could be attributed to the systemic effects. This difference in plasma aldosterone could explain many of the changes, especially with regard to ENaC. Compensatory mechanisms that could occur during development in the total *Nedd4L-Δ6-8* KO mice may also explain the difference with our inducible system. However, when we induced the renal *Nedd4L* deletion during embryonic development, we obtained a phenotype similar to that in the postnatal deletion of renal *Nedd4L*, with decreased plasma aldosterone, increased NCC, and decreased αENaC proteolysis. Therefore, the differences with the total *Nedd4L-Δ6-8* KO model could rather be due to variations in genetic background or to loss of nontubular NEDD4-2 function. Indeed, Van Huysse et al. recently demonstrated that the salt-induced elevated blood pressure in the *Nedd4L-Δ6-8* KO mouse model depends critically on ENaC overexpression in the brain (42).

Interestingly, despite the strong increase in renal NCC expression levels, the *Nedd4L*$^{Pax8/LC1}$ KO mice displayed some but not all the features characteristic of PHAII. The role of NCC overactivation in developing PHAII has been highlighted by human mutations and animal models. Wilson et al. first identified mutations in the *WNK1* and *WNK4* genes in some patients with PHAII (22). The PHAII-*Wnk4*^{Q562E} transgenic mouse model developed by Lalioti et al. exhibits increased NCC and PHAII features that could be abolished by crossing these mice with *Slc12a3* KO mice (33). Yang et al. generated mice with 1 normal copy of *Wnk4* and 1 mutant *Wnk4*^{D561A} (34). These mice displayed increased phosphorylation and expression of NCC as well as hypertension and hyperkalemia that could be treated with thiazide. However, there is now increasing evidence that overactive NCC alone is not sufficient to lead to PHAII and that the deregulation of other channels or transporters might be required. As mentioned above, *KS-Wnk1* KO mice, with strong increase in NCC and decreased ENaC, showed only few of the PHAII features (41). In addition, a recent study of NCC overexpression in mice showed no effect on blood pressure, plasma, or urine electrolyte and urinary Ca^{2+} (43). One of the PHAII features that is missing

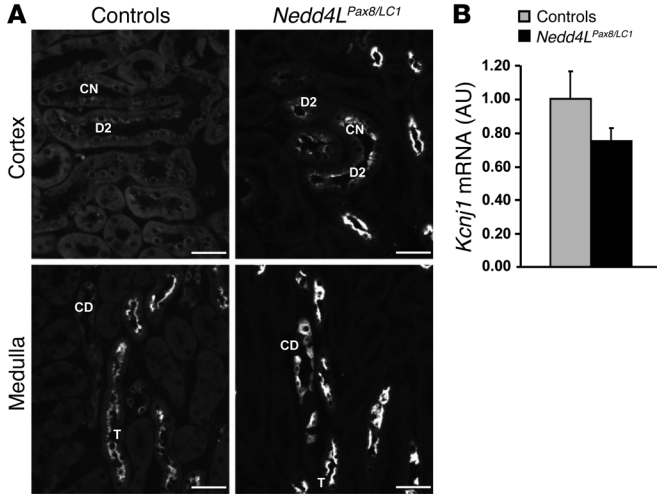

Figure 5
Nedd4L$^{Pax8/LC1}$ KO mice have increased ROMK abundance. (**A**) Immunofluorescence for ROMK on kidney sections from control and KO mice fed with high-Na$^+$ diet (10 days) shows increase in the channel in DCT2 (D2), CNT (CN), CD and TAL (T) in KO. Scale bars: ~40 μm. (**B**) TaqMan analysis showed that *Kcnj1* mRNA levels are not changed between controls and KO mice on whole kidney.

in the *Nedd4L*$^{Pax8/LC1}$ KO mice is the hyperkalemia. Several lines of evidence have shown that NCC is important for K$^+$ conservation, as Gitelman patients (44) and *Slc12a3* KO mice exhibit hypokalemia (45) and hyperkalemia is observed in PHAII patients (33, 34). The increased ROMK abundance observed in the *Nedd4L*$^{Pax8/LC1}$ KO mice, which could result from the lack of NEDD4-2–mediated ubiquitylation (46), may lead to higher K$^+$ excretion, as it has been reported for the *KS-Wnk1* KO mice (41). Another possibility could be that the *Nedd4L*$^{Pax8/LC1}$ KO mice have some residual ENaC activity sufficient for excreting enough K$^+$ to maintain a normal kalemia. Whether some ENaC-independent K$^+$ secretion occurs in the *Nedd4L*$^{Pax8/LC1}$ KO mice remains to be addressed.

In conclusion, we provide evidence that inactivation of *Nedd4L* exons 6 to 8 in renal tubules of adult mice does not lead to a Liddle syndrome phenotype associated with elevated ENaC activity, but rather causes a salt-sensitive PHAII-like syndrome with NCC upregulation, increased blood pressure, and hypercalciuria. Based on these results, NEDD4-2 appears to primarily target NCC and might thus be an attractive target to treat hypertension, avoiding the most severe side effect of thiazides, namely hypokalemia. Moreover, there is an interesting clinical association of hypercalciuria with hypertension and an increased risk of nephrolithiasis in hypertension (47–50). Defects in NEDD4-2 could therefore underlie these associations, and its study could lead to important mechanistic insights. The recent discoveries that mutations in *KLHL3* and *CUL3* (part of a ubiquitin-protein ligase complex) lead to PHAII demonstrate the importance of the ubiquitylation process in the control of NCC activation. In addition, Khan et al. very recently demonstrated that NCC ubiquitylation is regulated by phosphorylation of the cotransporter and may contribute to the control of NCC surface expression (51). Finally, our data suggest that under high-Na$^+$ intake, NEDD4-2 is not crucial for regulating renal ENaC, as the low plasma aldosterone leading to decreased αENaC proteolytic cleavage is probably sufficient to counterbalance the increased β- and γENaC abundance in the *Nedd4L*$^{Pax8/LC1}$ KO mice and thus to compensate for the increased NCC activity and maintain normal Na$^+$/K$^+$ balance. Why other pathways known to regulate NCC, such WNK-SPAK/OSR1, do not compensate for the increased NCC activity resulting from the lack of NEDD4-2 represents an important question for further investigation.

Methods

Generation and induction of renal tubule–specific Nedd4L KO mice. Inducible renal tubule–specific *Nedd4L*$^{flox/flox}$*/Pax8-rTA/LC1* KO (*Nedd4L*$^{Pax8/LC1}$) mice were generated as described previously (24). Genotyping and recombination of PCR were performed as described in Supplemental Methods. Three- to 4-week-old KO and single transgenic homozygous *Nedd4L*^{Pax8} or *Nedd4L*^{LC1} littermates (controls) were treated with doxycycline (2 mg/ml in 2% sucrose in drinking water) for 11 days. All experiments were started 1 day after the end of the induction, if not stated otherwise. To delete *Nedd4L* during embryonic development, pregnant females were treated with doxycycline as described above during the breeding and gestation periods, and resulting pups were treated until weaning. Induced mice were fed a standard (0.18% Na$^+$; Sniff) or high-Na$^+$ diet (>3.2% Na$^+$) for 8 days and placed in metabolic cages to measure BW, water, and food consumption and to collect urine for 24 hours. For thiazide treatment, mice were injected i.p. at Zeitgeber time ZT2 (2 hours after light on) with vehicle or thiazide (20 mg/kg BW) and urine was collected 6, 12, 24, and 30 hours after injection. Creatinine and Ca^{2+} were measured by the Laboratory of Clinical Chemistry at the Lausanne Hospital (CHUV) using a Modular

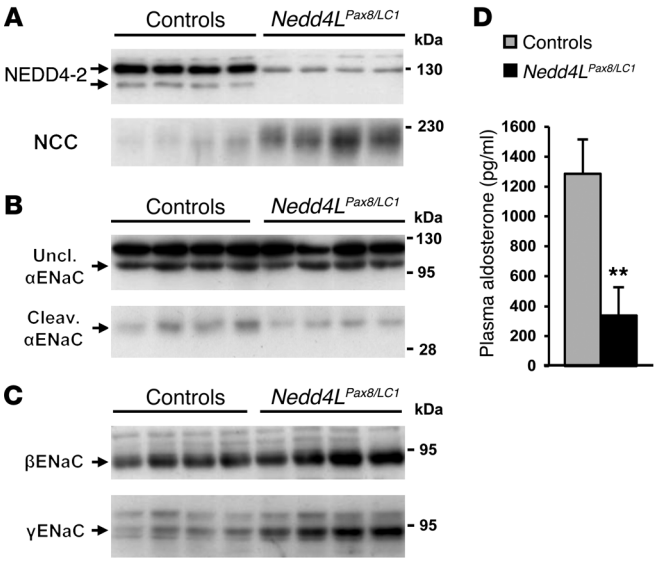

Figure 6
Nedd4L ablation in renal tubules during embryonic development results in phenotype similar to that seen when the deletion occurs at adult age. Mice were treated with doxycycline during embryonic development to induce *Nedd4L* ablation early on. (**A**–**C**) Western blot analysis on 5-week-old control and KO mice showed increased NCC (**A**), β-, and γENaC (**C**) expression, and decreased cleaved αENaC under high-Na$^+$ diet (10 days) (**B**). (**D**) Plasma aldosterone levels were decreased in KO (n = 7) compared with control mice (n = 7) under standard diet. *P < 0.05, KO versus controls.

Table 2
Urine and plasma electrolytes in controls and constitutive *Nedd4L*$^{Pax8/LC1}$ KO mice under high-Na$^+$ diet (8 days)

	Controls	*Nedd4L*$^{Pax8/LC1}$
Food intake (g/g BW/24 h)	0.20 ± 0.01 (9)	0.20 ± 0.01 (7)
Water intake (ml/g BW/24 h)	0.61 ± 0.06 (9)	0.67 ± 0.05 (6)
Urine		
Urine volume (ml/g BW/24 h)	0.23 ± 0.03 (9)	0.30 ± 0.02^A (7)
Ca^{2+} excretion (μmol/24 h)	13.5 ± 3.88 (9)	44.3 ± 7.16^B (7)
Ca^{2+}/Cr (10^3)	2.84 ± 0.52 (9)	7.50 ± 0.98^B (9)
Na^+ excretion (μmol/24 h)	2192 ± 232 (9)	2249 ± 279 (7)
Na^+/Cr (10^3)	0.66 ± 0.04 (9)	0.61 ± 0.06 (7)
K^+ excretion (μmol/24 h)	538 ± 40.0 (9)	639 ± 42.0 (7)
K^+/Cr (10^3)	0.16 ± 0.01 (9)	0.17 ± 0.01 (7)
Na^+/K^+	4.02 ± 0.20 (9)	3.49 ± 0.30 (7)
GFR (ml/g BW/24 h)	15.9 ± 1.38 (8)	15.6 ± 1.40 (5)
Plasma		
Na^+ (mM)	151 ± 0.47 (9)	152 ± 0.81 (7)
K^+ (mM)	4.20 ± 0.16 (9)	4.16 ± 0.20 (7)

Values are given as average ± SEM. Number of mice indicated in parentheses. $^AP < 0.05$, $^BP < 0.005$, KO versus controls.

Analytics System (Roche Diagnostics). Mice were anesthetized by isoflurane inhalation for blood collection by retroorbital plexus puncture and sacrificed by cervical dislocation for tissue collection.

Inducible renal tubule–specific Scnn1a KO mice. *Scnn1a*$^{flox/flox}$/Pax8-rTA/LC1 KO mice were generated and induced as described above for the *Nedd4L*$^{Pax8/LC1}$ KO mice, but using *Scnn1a*$^{flox/flox}$ mice (52).

Microdissection of mouse renal tubules. Kidneys were perfused and microdissected as described previously (53). For each tubular segment (PT, TAL, DCT, or CNT/CD), tubules microdissected from 3 mice were pooled together with equal tubular length (controls: 6–8 cm; KO: 12 cm to be sure not to miss any weak signal in comparison with controls).

Real-time quantitative PCR. Total RNA was isolated from kidney using the RNAquous Kit (Ambion) (1 μg) or from renal tubules microdissected as described in (53) using the RNeasy MicroKit (QIAGEN). RNA was reverse-transcribed and used for real-time quantitative PCR as described (24). Information about TaqMan Gene Expression Assays (Applied Biosystems) and primer/probe sequences are given in Supplemental Table 1. Regarding *Nedd4L*, the probe and primers were chosen to be located in the exon 6 to 8 region that was deleted in the KO mice after doxycycline treatment.

Measurement of urine and plasma metabolites and aldosterone. Urinary and plasma Na^+ and K^+ were measured using a flame photometer (Cole-Palmer Instrument), and urine osmolality with an Advanced 2020 osmometer (Advanced Instruments). Glomerular filtration rate (GFR) was estimated based on creatinine clearance. Plasma aldosterone levels were measured as described (24).

Telemetry. Experiments were performed on 1.5-month-old male controls and induced KO as described (41). Mice were fed a standard diet for 7 days, a low-Na$^+$ diet (<0.01% Na^+; Sniff) for 7 days, and then a high-Na$^+$ diet for up to 5 weeks. After a 10-day recovery period, cardiovascular parameters were recorded 9 seconds every minute for 24 hours in a light/dark-cycle (ZT0-ZT12/ZT12-ZT24). For thiazide and amiloride experiments, mice were injected i.p. with either vehicle, thiazide (20 mg/kg BW), or amiloride (5 mg/kg BW) at ZT11 and blood pressure was measured during the active night period between 2 hours (ZT13) and 9 hours (ZT20) after injection.

Aldosterone treatment. The ALZET 1003D osmotic mini-pumps (preloaded with vehicle or aldosterone to get a dose of 150 μg/kg BW/d for 3 days) were implanted s.c. Mice were kept on a low-Na$^+$ diet, from the implantation day until sacrifice, to avoid aldosterone escape.

Immunoblotting. Frozen tissues were homogenized and protein extracted as described (24). Anti–α-, –β-, and –γENaC were used as described (14). Kidneys from inducible renal tubule–specific *Scnn1a* KO mice were used as controls for the ENaC-specific bands. For analysis of protein expression in *Nedd4L* total KO mice, kidneys from P19 *Nedd4L-Δ15-16* total KO mice (31) were used. NEDD4-2 was detected using an anti–NEDD4-2 generated in the laboratory of S. Kumar and diluted 1/1000 (31) or with other antibodies directed against different regions of NEDD4-2 and described in Supplemental Methods. NEDD4-1 was detected as described in Supplemental Methods. NCC was detected with an anti-NCC antibody (Chemicon). For anti-phosphorylated pT53-NCC and pT58-NCC, peptide-synthesis, immunizations of rabbits, and antibody purifications were custom-made by Pineda Antibody Services. Phospho-antibodies were preincubated with the corresponding non–phospho-peptides and diluted 1/5000. Anti-phosphorylated pS71-NCC and anti-pT43/53/58-NCC were provided by D. Alessi (MRC Protein Phosphorylation Unit, University of Dundee, Dundee, United Kingdom) and preincubated with the corresponding non–phospho-peptide (35, 54). Anti–β-actin or anti–β-tubulin antibody (Sigma-Aldrich) was used as loading control. For protein analysis on microdissected renal tubules, Western blots were performed as described (53) using the NEDD4-2 antibody previously described (31).

Immunofluorescence. Kidneys were processed and cryosections incubated with antibodies against CRE, α-, β-, γENaC, NCC, and ROMK1,2 as described (15, 55).

Statistics. All values are presented as mean ± SEM. The data were analyzed using unpaired 2-tailed Student's *t* test, KO versus controls. For thiazide and amiloride injection, a paired *t* test was used, diuretic injected versus vehicle injected. A *P* value of less than 0.05 was considered significant.

Study approval. All experimental procedures were approved by the Swiss Federal Veterinary Office and carried out in accordance with the local animal welfare act.

Acknowledgments

We thank J.P. Arroyo, O. Bonny, N. Faresse, G. Gamba, D. Pouly, R.D. Rajuram, B. Rossier, and L. Schild for critically reading the manuscript. We are very thankful to R. Garcia Barros and M. Stifanelli for their technical assistance. This work was supported by the Leducq Foundation Transatlantic Network on Hypertension (to O. Staub and E. Hummler), the Swiss National Science Foundation 310030-141013 (to O. Staub), 310030-122243 (to J. Loffing) and 3100A0-102125/1 (to E. Hummler), the Swiss NCCR Kidney.ch (to O. Staub, J. Loffing, and E. Hummler), the Swiss Kidney Foundation (to C. Ronzaud), and National Health and Medical Research Council grant APP1020755 and fellowship 1002863 (to N.A. Boase and S. Kumar).

Received for publication August 13, 2012, and accepted in revised form November 16, 2012.

Address correspondence to: Oliver Staub, Department of Pharmacology and Toxicology, University of Lausanne, Rue du Bugnon 27, 1005 Lausanne, Switzerland. Phone: 41.21.692.5407; Fax: 41.21.692.5355; E-mail: olivier.staub@unil.ch. Or to: Johannes Loffing, Institute of Anatomy, University of Zurich, Winterthurerstrasse 190, 8057 Zurich, Switzerland. Phone: 41.44.635.5320; Fax: 41.44.635.5702; E-mail: johannes.loffing@anatom.uzh.ch.

1. Reilly RF, Ellison DH. Mammalian distal tubule: physiology, pathophysiology, and molecular anatomy. *Physiol Rev*. 2000;80(1):277–313.
2. Giebisch G. Renal potassium transport: mechanisms and regulation. *Am J Physiol*. 1998; 274(5 pt 2):F817–F833.
3. Shimkets RA, et al. Liddle's syndrome: heritable human hypertension caused by mutations in the β subunit of the epithelial sodium channel. *Cell*. 1994;79(3):407–414.
4. Snyder PM, Steines JC, Olson DR. Relative contribution of Nedd4 and Nedd4-2 to ENaC regulation in epithelia determined by RNA interference. *J Biol Chem*. 2004;279(6):5042–5046.
5. Staub O, et al. WW domains of Nedd4 bind to the proline-rich PY motifs in the epithelial Na^+ channel deleted in Liddle's syndrome. *EMBO J*. 1996;15(10):2371–2380.
6. Kamynina E, Debonneville C, Bens M, Vandewalle A, Staub O. A novel mouse Nedd4 protein suppresses the activity of the epithelial Na^+ channel. *FASEB J*. 2001;15(1):204–214.
7. Abriel H, et al. Defective regulation of the epithelial Na^+ channel (ENaC) by Nedd4 in Liddle's syndrome. *J Clin Invest*. 1999;103(5):667–673.
8. Harvey KF, Dinudom A, Cook DI, Kumar S. The Nedd4-like protein KIAA0439 is a potential regulator of the epithelial sodium channel. *J Biol Chem*. 2001;276(11):8597–8601.
9. Debonneville C, et al. Phosphorylation of Nedd4-2 by Sgk1 regulates epithelial Na(+) channel cell surface expression. *EMBO J*. 2001;20(24):7052–7059.
10. Hughey RP, et al. Maturation of the epithelial Na+ channel involves proteolytic processing of the α- and γ-subunits. *J Biol Chem*. 2003;278(39):37073–37082.
11. Masilamani S, Kim G-H, Mitchell C, Wade JB, Knepper MA. Aldosterone-mediated regulation of ENaC α, β, and γ subunit proteins in rat kidney. *J Clin Invest*. 1999;104(7):R19–R23.
12. Rossier BC, Stutts MJ. Activation of the epithelial sodium channel (ENaC) by serine proteases. *Annu Rev Physiol*. 2009;71:361–379.
13. Canessa CM, et al. Amiloride-sensitive epithelial Na^+ channel is made of three homologous subunits. *Nature*. 1994;367(6462):463–467.
14. Rubera I, et al. Collecting duct-specific gene inactivation of αENaC in the mouse kidney does not impair sodium and potassium balance. *J Clin Invest*. 2003;112(4):554–565.
15. Ronzaud C, et al. Impairment of sodium balance in mice deficient in renal principal cell mineralocorticoid receptor. *J Am Soc Nephrol*. 2007;18(6):1679–1687.
16. Gamba G. Molecular physiology and pathophysiology of electroneutral cation-chloride cotransporters. *Physiol Rev*. 2005;85(2):423–493.
17. Wilson FH, et al. Molecular pathogenesis of inherited hypertension with hyperkalemia: the Na-Cl cotransporter is inhibited by wild-type but not mutant WNK4. *Proc Natl Acad Sci U S A*. 2003;100(2):680–684.
18. Yang CL, Angell J, Mitchell R, Ellison DH. WNK kinases regulate thiazide-sensitive Na-Cl cotransport. *J Clin Invest*. 2003;111(7):1039–1045.
19. Louis-Dit-Picard H, et al. KLHL3 mutations cause familial hyperkalemic hypertension by impairing ion transport in the distal nephron. *Nat Genet*. 2012;44(4):456–460.
20. Boyden LM, et al. Mutations in kelch-like 3 and cullin 3 cause hypertension and electrolyte abnormalities. *Nature*. 2012;482(7383):98–102.
21. Faresse N, et al. Inducible kidney-specific Sgk1 knockout mice show a salt-losing phenotype. *Am J Physiol Renal Physiol*. 2012;302(8):F977–F985.
22. Wilson FH, et al. Human hypertension caused by mutations in WNK kinases. *Science*. 2001; 293(5532):1107–1112.
23. Mayan H, Vered I, Mouallem M, Tzadok-Witkon M, Pauzner R, Farfel Z. Pseudohypoaldosteronism type II: marked sensitivity to thiazides, hypercalciuria, normomagnesemia, and low bone mineral density. *J Clin Endocrinol Metab*. 2002;87(7):3248–3254.
24. Arroyo JP, et al. Nedd4-2 Modulates Renal Na+-Cl- Cotransporter via the Aldosterone-SGK1-Nedd4-2 Pathway. *J Am Soc Nephrol*. 2011;22(9):1707–1719.
25. Shi PP, et al. Salt-sensitive hypertension and cardiac hypertrophy in mice deficient in the ubiquitin ligase Nedd4-2. *Am J Physiol Renal Physiol*. 2008;295(2):F462–F470.
26. Loffing-Cueni D, et al. Dietary sodium intake regulates the ubiquitin-protein ligase nedd4-2 in the renal collecting system. *J Am Soc Nephrol*. 2006;17(5):1264–1274.
27. Traykova-Brauch M, et al. An efficient and versatile system for acute and chronic modulation of renal tubular function in transgenic mice. *Nat Med*. 2008;14(9):979–984.
28. Kamynina E, Tauxe C, Staub O. Differential characteristics of two human Nedd4 proteins with respect to epithelial Na^+ channel regulation. *Am J Physiol*. 2001;281:F469–F477.
29. Ruffieux-Daidie D, Poirot O, Boulkroun S, Verrey F, Kellenberger S, Staub O. Deubiquitylation regulates activation and proteolytic cleavage of ENaC. *J Am Soc Nephrol*. 2008;19(11):2170–2180.
30. Pacheco-Alvarez D, et al. The Na+:Cl- cotransporter is activated and phosphorylated at the amino-terminal domain upon intracellular chloride depletion. *J Biol Chem*. 2006;Na(39):28755–28763.
31. Boase NA, et al. Respiratory distress and perinatal lethality in Nedd4-2-deficient mice. *Nat Commun*. 2011;2:287.
32. Loffing J, et al. Altered renal distal tubule structure and renal Na(+) and Ca(2+) handling in a mouse model for Gitelman's syndrome. *J Am Soc Nephrol*. 2004;15(9):2276–2288.
33. Lalioti MD, et al. Wnk4 controls blood pressure and potassium homeostasis via regulation of mass and activity of the distal convoluted tubule. *Nat Genet*. 2006;38(10):1124–1132.
34. Yang SS, et al. Molecular pathogenesis of pseudohypoaldosteronism type II: generation and analysis of a Wnk4(D561A/+) knockin mouse model. *Cell Metab*. 2007;5(5):331–344.
35. Richardson C, et al. Activation of the thiazide-sensitive Na+-Cl- cotransporter by the WNK-regulated kinases SPAK and OSR1. *J Cell Sci*. 2008; 121(pt 5):675–684.
36. Asher C, Wald H, Rossier BC, Garty H. Aldosterone-induced increase in the abundance of Na+ channel subunits. *Am J Physiol*. 1996;271(2 pt 1):C605–C611.
37. Rubera I, et al. Collecting duct-specific gene inactivation of alphaENaC in the mouse kidney does not impair sodium and potassium balance. *J Clin Invest*. 2003;112(4):554–565.
38. Pradervand S, et al. Dysfunction of the epithelial sodium channel expressed in the kidney of a mouse model for Liddle syndrome. *J Am Soc Nephrol*. 2003;14(9):2219–2228.
39. Staub O, Rotin D. Role of ubiquitylation in cellular membrane transport. *Physiol Rev*. 2006;86(2):669–707.
40. Brooks HL, et al. Profiling of renal tubule Na+ transporter abundances in NHE3 and NCC null mice using targeted proteomics. *J Physiol*. 2001;530(pt 3):359–366.
41. Hadchouel J, et al. Decreased ENaC expression compensates the increased NCC activity following inactivation of the kidney-specific isoform of WNK1 and prevents hypertension. *Proc Natl Acad Sci U S A*. 2010;107(42):18109–18114.
42. Van Huysse JW, Amin MS, Yang B, Leenen FH. Salt-induced hypertension in a mouse model of liddle syndrome is mediated by epithelial sodium channels in the brain. *Hypertension*. 2012;60(3):691–696.
43. McCormick JA, Nelson JH, Yang CL, Curry JN, Ellison DH. Overexpression of the sodium chloride cotransporter is not sufficient to cause familial hyperkalemic hypertension. *Hypertension*. 2011;58(5):888–894.
44. Simon DB, et al. Gitelman's variant of Bartter's syndrome, inherited hypokalaemic alkalosis, is caused by mutations in the thiazide-sensitive Na-Cl cotransporter. *Nat Genet*. 1996;12(1):24–30.
45. Morris RG, Hoorn EJ, Knepper MA. Hypokalemia in a mouse model of Gitelman's syndrome. *Am J Physiol Renal Physiol*. 2006;290(6):F1416–F1420.
46. Lin DH, et al. POSH stimulates the ubiquitination and the clathrin-independent endocytosis of ROMK1 channels. *J Biol Chem*. 2009; 284(43):29614–29624.
47. Khan SR. Is oxidative stress, a link between nephrolithiasis and obesity, hypertension, diabetes, chronic kidney disease, metabolic syndrome? *Urol Res*. 2012;40(2):95–112.
48. Cupisti A. Update on nephrolithiasis: beyond symptomatic urinary tract obstruction. *J Nephrol*. 2011;18:S25–S29.
49. Reilly RF, Peixoto AJ, Desir GV. The evidence-based use of thiazide diuretics in hypertension and nephrolithiasis. *Clin J Am Soc Nephrol*. 2010;5(10):1893–1903.
50. Obligado SH, Goldfarb DS. The association of nephrolithiasis with hypertension and obesity: a review. *Am J Hypertens*. 2008;21(3):257–264.
51. Hossain Khan MZ, et al. Phosphorylation of Na-Cl cotransporter by OSR1 and SPAK kinases regulates its ubiquitination. *Biochem Biophys Res Commun*. 2012;425(2):456–461.
52. Hummler E, et al. Early death due to defective neonatal lung liquid clearance in alpha-ENaC-deficient mice. *Nat Genet*. 1996;12(3):325–328.
53. Christensen BM, et al. Sodium and potassium balance depends on alphaENaC expression in connecting tubule. *J Am Soc Nephrol*. 2010;21(11):1942–1951.
54. Rafiqi FH, et al. Role of the WNK-activated SPAK kinase in regulating blood pressure. *EMBO Mol Med*. 2010;2(2):63–75.
55. Wagner CA, et al. Mouse model of type II Bartter's syndrome. II. Altered expression of renal sodium- and water-transporting proteins. *Am J Physiol Renal Physiol*. 2008;294:F1373–F1380.